数理解析研究所講究録
第 1699 巻 2010 年 1-12

Family of Julia sets as Orbits of Differential Equations

Yi-Chiuan Chen*†‡
Institute of Mathematics, Academia Sinica

Key words: Julia set, Mandelbrot set, symbolic dynamics, anti-integrable limit
2000 Mathematics Subject Classification: 37F10, 37F45, 37F50

1 Introduction

This note is based on a talk the author gave at the RIMS conference.

Every complex quadratic polynomial map $z \mapsto az^2 + bz + d$ (a, b, $d \in \mathbb{C}$, $a \neq 0$) can be put into a normal form $q_c : z \mapsto z^2 + c$, with z, $c \in \mathbb{C}$. Another well-known normal form is the logistic map $f_\mu : z \mapsto \mu z(1-z)$, with z, $\mu \in \mathbb{C}$, which is conjugate to q_c via the conjugacy

$$h : z \mapsto -\mu z + \mu/2 \tag{1}$$

with $c = \mu(2-\mu)/4$ and $\mu \neq 0$. Hence, we can freely employ either form q_c or f_μ for investigation of quadratic holomorphic maps.

By $K(q_c)$ we denote the *filled Julia set* of the map q_c,

$$K(q_c) := \{z |\ q_c^n(z),\ n \geq 0,\ \text{is bounded}\},$$

then the *Julia set* $J(q_c)$ of q_c is the boundary of the filled Julia set,

$$J(q_c) := \partial K(q_c).$$

*Postal address: 6F of Astronomy-Mathematics Building, No. 1, Sec. 4, Roosevelt Road, Taipei 10617, Taiwan, ROC
†Email: YCChen@math.sinica.edu.tw
‡Supported by NSC 98-2115-M-001-012.

The famous *Mandelbrot set* for q_c is defined to be

$$M_c := \{c|\ q_c^n(0),\ n \geq 0,\ \text{is bounded}\}.$$

Similarly, we use $K(f_\mu)$, $J(f_\mu)$, and

$$M_\mu := \{\mu|\ f_\mu^n(1/2),\ n \geq 0,\ \text{is bounded}\}$$

to denote the filled Julia set, the Julia set, and the Mandelbrot set of f_μ, respectively.

The Julia set for μ not belonging to the Mandelbrot set is hyperbolic, thus varies continuously when parameter μ changes (e.g. [12, 14]). It follows that a continuous curve in the exterior of the Mandelbrot set induces a continuous family of Julia sets. In this note, we are concerned with the fact that this family is governed by an infinitely coupled differential equations (see (3) below) that the author obtained recently in [6]. This approach may bring new insights into the study of dynamical systems.

The continuous family of Julia sets $J(f_\mu)$ when parameter μ varies from infinity along an external ray of the Mandelbrot set M_μ to a Misiurewicz point hence can be realized as an orbit of the infinitely coupled differential equations (3) integrated along the external ray. We use the OTIS algorithm [11] to obtain numerical data of the external rays.

2 Conjugacy via the anti-integrability

Let $l_\infty := \{\mathbf{z}|\ \mathbf{z} = \{z_i\},\ i \in \mathbb{N}\}$ endowed with the sup norm be the Banach space of bounded sequences in $\mathbb{C}$. Rewrite the logistic map $z_i \mapsto z_{i+1} = \epsilon^{-1} z_i(1 - z_i)$, $i \geq 0$, as

$$\begin{aligned} F : l_\infty \times \mathbb{C} &\to l_\infty, \\ (\mathbf{z}, \epsilon) &\mapsto F(\mathbf{z}, \epsilon) = \{F_0(\mathbf{z}, \epsilon), F_1(\mathbf{z}, \epsilon), F_2(\mathbf{z}, \epsilon), \ldots\} \end{aligned}$$

with $F_i(\mathbf{z}, \epsilon) = -\epsilon z_{i+1} + z_i(1 - z_i)$, then the anti-integrability for the logistic map can be formulated by five steps [1, 3, 4, 13] which in the current context are described by the following five propositions [4, 5]:

Proposition 1. *(i) When $\epsilon \neq 0$, $\mathbf{z}$ is a bounded orbit of $f_{1/\epsilon}$ if and only if $F(\mathbf{z}, \epsilon) = 0$. (ii) $F(\mathbf{z}^\dagger, 0) = 0$ if and only if $z_i^\dagger = 0$ or 1 for every $i \geq 0$.*

Proposition 2. *Let $\Sigma \subset \mathbb{C}^{\mathbb{N}}$ be the set constituting all such $\mathbf{z}^\dagger$'s, then Σ with the product topology is a Cantor set.*

The map F is C^1, and $D_{\mathbf{z}}F(\mathbf{z},\epsilon)$ is invertible if and only if

$$-\epsilon\xi_{i+1} + (1-2z_i)\xi_i = \eta_i \tag{2}$$

possesses a unique bounded solution for any given $\eta = \{\eta_i\}_{i\geq 0} \in l_\infty$. The solution

$$\xi_i = \sum_{N\geq 0} \epsilon^N \left(\prod_{k=0}^{N} (1-2z_{i+k})^{-1}\right) \eta_{i+N}$$

is bounded for every $i \geq 0$ because it can be bounded by a geometric series due to the expanding property of the Julia set when $\epsilon \notin M_\mu^{-1}$. (The "inside-out" Mandelbrot set M_μ^{-1} is defined by

$$M_\mu^{-1} := \{1/\mu |\ \mu \in M_\mu\}.)$$

The homogeneous solution of (2),

$$\xi_{i+N} = \xi_i \epsilon^{-N} \prod_{k=0}^{N-1} (1-2z_{i+k}) \quad \forall\, i \geq 0,\ N \geq 1,$$

by the same expanding property, is unbounded unless ξ is identical to 0. This means the solution above is the only bounded solution.

Proposition 3. *The orbit* $\mathbf{z}^*$ *is a solution of the following functional differential equation*

$$D\mathbf{z}(\epsilon) = -D_{\mathbf{z}}F(\mathbf{z}(\epsilon),\epsilon)^{-1}\ D_\epsilon F(\mathbf{z}(\epsilon),\epsilon),$$

and hence satisfies a system of infinitely coupled differential equations

$$\frac{d}{d\epsilon} z_n = \sum_{N\geq 0} \epsilon^N \left(\prod_{k=0}^{N} (1-2z_{n+k})^{-1}\right) z_{n+1+N}. \tag{3}$$

The crucial issue is how to solve (3). We shall treat it as the initial value problem, with initial values specified at $\epsilon = 0$. As ϵ approaches zero, the set of bounded orbits $\{z_n^*(\epsilon)\}_{n\geq 0}$ of the map $f_{1/\epsilon}$ converges to the set Σ. This indicates that for every $n \geq 0$ there are exactly two possibilities for the initial conditions of (3): $z_n^*(0) = 0$ or $z_n^*(0) = 1$.

Proposition 4.

$$J(f_{1/\epsilon}) = \bigcup_{\mathbf{z}^\dagger\in\Sigma} \pi \circ g_\epsilon(\mathbf{z}^\dagger),$$

in which

$$\mathbf{z}^\dagger \xmapsto{g_\epsilon} \mathbf{z}^*(\epsilon;\mathbf{z}^\dagger) \xmapsto{\pi} z_0^*(\epsilon;\mathbf{z}^\dagger),$$

where π *is the projection* $\mathbf{z} = (z_0, z_1, \cdots) \mapsto z_0 \in \mathbb{C}$.

Remark 5. With the product topology, the mapping $g_\epsilon : \mathbf{z}^\dagger \mapsto \mathbf{z}^*(\epsilon; \mathbf{z}^\dagger)$ is continuous [3, 4, 5].

Proposition 6. *Providing $\epsilon \notin M_\mu^{-1}$, the following diagram commutes:*

$$\begin{array}{ccc} \Sigma & \xrightarrow{\sigma} & \Sigma \\ {\scriptstyle \pi\circ g_\epsilon}\big\downarrow & & \big\downarrow{\scriptstyle \pi\circ g_\epsilon} \\ J(f_{1/\epsilon}) & \xrightarrow{f_{1/\epsilon}} & J(f_{1/\epsilon}). \end{array}$$

Remark 7. The advantage of our approach is that the conjugacy comes automatically and can be realized explicitly as $\pi \circ g_\epsilon$. In fact, g_ϵ is realized as the solutions of the initial value problems for the infinitely coupled differential equations (3).

3 Continuation from the anti-integrable limit

We can assign each point in the Julia set a *symbolic code* by virtue of the one-to-one correspondence between $J(q_c)$ and Σ. But, there is no unique way to assign the code. One example of such a coding is the *itinerary sequence*. Below we recall the canonical potential function associated with the filled Julia set in order to see how an itinerary sequence can be assigned and, at the same time, to introduce some notations. (See, for example, [2, 9, 10, 15, 16].)

Let $\beta = 1/c$. The dynamical behavior of q_c near infinity can be understood by making the substitution $\zeta = 1/z$ and considering the rational function

$$Q_\beta(\zeta) := \frac{1}{q_{1/\beta}(1/\zeta)}.$$

The associated Böttcher map ϕ_β defined by

$$\phi_\beta(\zeta) := \lim_{n\to\infty} \sqrt[2^n]{Q_\beta^n(\zeta)}$$

carries an open subset of the immediate basin of the fixed point 0 biholomorphically onto an open disc $\mathbb{D}_r$ of radius r, $0 < r \leq 1$, centred at the origin. If $\beta \notin M_c^{-1}$, where

$$M_c^{-1} := \{1/c|\ c \in M_c\},$$

then $r = \lim_{\zeta\to\infty} |\phi_\beta(\zeta)| < 1$ and $\phi_\beta^{-1}(\mathbb{D}_r) = \{\zeta|\ |\phi_\beta(\zeta)| < r\}$. The map $\hat{\phi}_c$ defined by the reciprocal

$$\hat{\phi}_c(z) := \frac{1}{\phi_{1/c}(1/z)} = \lim_{n\to\infty} \sqrt[2^n]{q_c^n(z)}$$

maps biholomorphically from the open set $\{z|\ G_c(z) > G_c(0)\} \subseteq \mathbb{C} \setminus K(q_c)$ to the region $\mathbb{C} \setminus \bar{\mathbb{D}}_{\hat{r}} = \{w|\ \ln|w| > G_c(0)\}$, where $\hat{r} = |\hat{\phi}_c(0)| > 1$ and $G_c : \mathbb{C} \longrightarrow [0, \infty)$, defined by

$$G_c(z) := \ln^+ |\hat{\phi}_c(z)| = \lim_{n\to\infty} \frac{1}{2^n} \ln^+ |q_c^n(z)|, \qquad (\ln^+ |w| = \max\{\ln|w|, 0\})$$

is the *canonical potential function* associated with the filled Julia set $K(q_c)$. The map $\hat{\phi}_c$ is a conjugacy between q_c on $\{z|\ G_c(z) > G_c(0)\}$ and $w \mapsto w^2$ on $\{w|\ \ln|w| > G_c(0)\}$.

For $\theta \in \mathbb{R}/\mathbb{Z}$, define the *external ray* $\mathcal{R}(\theta; K(q_c))$ of angle θ of the filled Julia set $K(q_c)$ by

$$\mathcal{R}(\theta; K(q_c)) := \{\hat{\phi}_c^{-1}(re^{i2\pi\theta})|\ |\hat{\phi}_c(0)| < r \leq \infty\}. \tag{4}$$

The critical value $c \in \mathbb{C} \setminus K(q_c)$ has a well defined external angle when $c \notin M_c$. Let it be denoted by $l(c) \in \mathbb{R}/\mathbb{Z}$, given by $c = \hat{\phi}_c^{-1}(|\hat{\phi}_c(c)|e^{i2\pi l(c)})$. The ray $\mathcal{R}(l(c); K(q_c))$ has two preimages, $\mathcal{R}(l(c)/2; K(q_c))$ and $\mathcal{R}((l(c)+1)/2; K(q_c))$. These two together with the origin separate $\bar{\mathbb{C}}$ into two disjoint open sets, say V_0 and V_1. These constitute a *Markov partition.* That is to say, for any infinite sequence $(b_0, b_1, \dots) \in \Sigma$, there exists one and only one point $z \in K(q_c)$ with $q_c^i(z) \in V_{b_i}$ for every $i \geq 0$. However, there is ambiguity in determining which open set should be labeled by V_0 and which by V_1. In Definition 8, we shall define the itinerary sequences used in this note for points in the Julia set $J(f_\mu)$. Our definition arises very naturally from the viewpoint of the system's anti-integrable limit.

By using (1), define

$$\mathcal{R}(\theta; K(f_\mu)) := h^{-1}(\mathcal{R}(\theta; K(q_c))).$$

The two external rays $\mathcal{R}(l(c)/2; K(f_{1/\epsilon}))$ and $\mathcal{R}((l(c)+1)/2; K(f_{1/\epsilon}))$, which land at the point $z = 1/2$, divide the complex plane into two partitions, one containing the fixed point 0, the other containing the other fixed point $1-\epsilon$.

Definition 8. Assume $z_{n+1} = f_{1/\epsilon}(z_n)$ for all $n \geq 0$. Suppose $\{z_n\}_{n\geq 0}$ is bounded and is bounded away from the two dynamic rays that land at $1/2$. Define its *itinerary sequence* $\{\alpha_n\}_{n\geq 0}$ as follows: $\alpha_n = 0$ if z_n is located in the same open set as the fixed point 0 is; $\alpha_n = 1$ if z_n is located in the same open set as the fixed point $1-\epsilon$ is.

Theorem 9. *Suppose $0 \neq \hat{\epsilon} \notin M_\mu^{-1}$ and suppose $\{z_n\}_{n\geq 0}$, with $z_n = f_{1/\hat{\epsilon}}^n(z_0)\ \forall\ n \geq 0$, is a bounded orbit of the logistic map $f_{1/\hat{\epsilon}}$ with itinerary sequence $\{\alpha_n\}_{n\geq 0}$. Assume $z_n^*(\epsilon)$ is the solution of (3) integrated along an integral curve in $\bar{\mathbb{C}} \setminus M_\mu^{-1}$ connecting $\epsilon = 0$ to $\epsilon = \hat{\epsilon}$ subject to initial condition $z_n^*(0) = \alpha_n$ for every $n \geq 0$. Then the value of $z_n^*(\hat{\epsilon})$ is independent of integral curves, and $z_n^*(\hat{\epsilon}) = z_n$ for all n.*

If $\{z_n\}$, $n \geq 0$, is a period-$(p+1)$ orbit of $f_{1/\epsilon}$ with itinerary $\{\overline{\alpha_0\alpha_1\ldots\alpha_p}\}$, then $z_n^*(\epsilon)$ can be obtained by integrating a $(p+1)$-coupled ODEs of the form

$$\frac{d}{d\epsilon}z_n = \left(1-\epsilon^{p+1}\prod_{k=0}^{p}(1-2z_{n+k})^{-1}\right)^{-1}\sum_{N=0}^{p}\epsilon^N\left(\prod_{k=0}^{N}(1-2z_{n+k})^{-1}\right)z_{n+1+N} \tag{5}$$

with the periodicity $z_{n+1+p} = z_n$ and initial condition $z_n^*(0) = \alpha_n$ for every $0 \leq n \leq p$ (see [6]). This provides a way for finding all roots of a class of polynomials. Suppose we are interested in finding all periodic orbits of the map $z \mapsto \epsilon^{-1}z(1-z)$. What we usually do is to solve a polynomial of 2^{p+1}-degree for z_0 arising from the following algebraic relation: $z_1 = \epsilon^{-1}z_0(1-z_0)$, $z_2 = \epsilon^{-1}z_1(1-z_1)$, $\ldots$, $z_p = \epsilon^{-1}z_{p-1}(1-z_{p-1})$, $z_0 = \epsilon^{-1}z_p(1-z_p)$. If $0 \neq \epsilon \notin M_\mu^{-1}$, we know that the polynomial for z_0 has 2^{p+1} distinct roots, corresponding to 2^{p+1} distinct initial points for all of period-2^{p+1} orbits (not all are of least period). Even if we find all roots of the polynomial, another question that concerns distinguishing the combinatorics of these roots is the itinerary of their corresponding orbits.

Corollary 10. *Let $0 \neq \hat{\epsilon} \notin M_\mu^{-1}$. Assume $\tilde{z}_0$ is one root of the aforementioned 2^{p+1}-degree polynomial for z_0 with $\epsilon = \hat{\epsilon}$ and the itinerary of its orbit is $\alpha = \{\alpha_n\}_{n\geq 0}$. Then $\tilde{z}_0$ can be obtained by integrating the $(p+1)$-coupled ODEs, namely $\tilde{z}_0 = z_0^*(\hat{\epsilon};\alpha)$.*

Because for every $n \geq 0$ the solution $z_n^*(\epsilon)$ of (3) depends continuously on ϵ and has to be bounded away from the two dynamic rays, the itinerary sequence of $\{z_n^*(\epsilon)\}_{n\geq 0}$ is equal to $\{z_n^*(0)\}_{n\geq 0}$.

Once initial conditions $z_n^*(\epsilon = 0)$ for all $n \geq 0$ are given, the value of the solution $z_n^*(\epsilon)$ of (3) at $\epsilon = \hat{\epsilon} \in \bar{\mathbb{C}} \setminus M_\mu^{-1}$ depends only on $\hat{\epsilon}$. Because $\hat{\epsilon}$ may locate arbitrarily close to ∂M_μ^{-1}, we have to specify an integral curve that can approach as close as possible to the boundary ∂M_μ^{-1}. This can be done if the integral curve we employ is an external ray.

Define

$$\hat{\Phi}_n(c) := \sqrt[2^n]{q_c^n(c)} \tag{6}$$

in $\bar{\mathbb{C}} \setminus M_c$ by the branch $\hat{\Phi}_n(c) = c + O(1)$ as $c \to \infty$. The sequence $\hat{\Phi}_n$ converges as $n \to \infty$ uniformly on compact subsets of $\bar{\mathbb{C}} \setminus M_c$ to the function $\hat{\Phi}$ with $\hat{\Phi}(c) \equiv \hat{\phi}_c(c)$, which is biholomorphic from $\bar{\mathbb{C}} \setminus M_c$ to $\bar{\mathbb{C}} \setminus \bar{\mathbb{D}}_1$, and the inverse $\hat{\Phi}_n^{-1}$ converges to $\hat{\Phi}^{-1}$ uniformly on compact subsets of $\bar{\mathbb{C}} \setminus \bar{\mathbb{D}}_1$. For $\theta \in \mathbb{R}/\mathbb{Z}$, the set

$$\mathcal{R}(\theta; M_c) := \{\hat{\Phi}^{-1}(re^{i2\pi\theta})|\ 1 < r \leq \infty\}$$

is called the *external ray* of angle θ of the Mandelbrot sets M_c. In contrast to $\hat{\Phi}^{-1}$, the map Φ^{-1} defined by

$$\Phi^{-1}(w) := \frac{1}{\hat{\Phi}^{-1}(1/w)} \tag{7}$$

is a biholomorphism of $\mathbb{D}_1$ onto $\bar{\mathbb{C}} \setminus M_c^{-1}$.

Suppose $\beta \notin M_c^{-1}$ and $\Phi(\beta) = w \in \mathbb{D}_1$. The relation between β and ϵ is

$$\beta = \frac{4\epsilon^2}{2\epsilon - 1},$$

in particular, $\beta = -4\epsilon^2 + O(\epsilon^3)$ when ϵ is small. By the Riemann Mapping Theorem, there exists a unique biholomorphic map

$$\Psi : \bar{\mathbb{C}} \setminus M_\mu^{-1} \longrightarrow \mathbb{D}_1$$

satisfying $\Psi(0) = 0$ and $\Psi(\epsilon) = -2i\epsilon + O(\epsilon^2)$ when ϵ is small. Consequently, the following diagram commutes

$$\begin{tikzcd}
\epsilon \in \bar{\mathbb{C}} \setminus M_\mu^{-1} \arrow[r, "\Psi"] \arrow[d] \arrow[dr, "\Upsilon"] & \mathbb{D}_1 \arrow[r] \arrow[d, "\Psi(\epsilon)\mapsto(\Psi(\epsilon))^2"] & \bar{\mathbb{C}} \setminus M_\mu \ni \mu \arrow[d] \\
\beta \in \bar{\mathbb{C}} \setminus M_c^{-1} \arrow[r, "\Phi"'] & \mathbb{D}_1 \arrow[r, "\hat{\Phi}^{-1}(1/\cdot)"'] & \bar{\mathbb{C}} \setminus M_c \ni c.
\end{tikzcd}$$

In the diagram the map $\Upsilon : \bar{\mathbb{C}} \setminus M_\mu^{-1} \longrightarrow \mathbb{D}_1$, $\epsilon \longmapsto w$, is defined by

$$\Upsilon(\epsilon) = (\Psi(\epsilon))^2 = w.$$

Using $w = re^{i2\pi\theta}$, $0 \leq r < 1$, $0 \leq \theta < 1$, we specify the two branches $\Upsilon_\pm^{-1}$ of the inverse of Υ as the following:

$$\Upsilon_\pm^{-1}(re^{i2\pi\theta}) := \Psi^{-1}(\pm\sqrt{r}e^{i\pi\theta}). \tag{8}$$

Our integral curves for (3) are external rays of M_μ^{-1}. For $\theta \in \mathbb{R}/\mathbb{Z}$, define the two *external rays* $\mathcal{R}^+(\theta; M_\mu^{-1})$ and $\mathcal{R}^-(\theta; M_\mu^{-1})$ of angle θ of M_μ^{-1} by

$$\begin{aligned}
\mathcal{R}^+(\theta; M_\mu^{-1}) &:= \{\Upsilon_+^{-1}(re^{-i2\pi\theta}) |\ 0 \leq r < 1\}, \\
\mathcal{R}^-(\theta; M_\mu^{-1}) &:= \{\Upsilon_-^{-1}(re^{-i2\pi\theta}) |\ 0 \leq r < 1\}.
\end{aligned}$$

4 Two examples

We use finitely many points that constitute an invariant subset to approximate the Julia set. Consequently the infinitely coupled differential equations (3) become a finitely coupled ODEs. In this section, examples of a periodic orbit and an eventually periodic orbit are demonstrated. See [8] for more examples.

4.1 External angle 1/6

We choose the initial conditions $\{z_0^*(0), z_1^*(0), \ldots, z_m^*(0), 1, \overline{10}\}$ with $z_n^*(0) \in \{0,1\}$ for all $0 \le n \le m$ to deal with (3). The initial condition in this case indicates that, after $m+2$ times iterations, orbits will become periodic with period 2. That is, $z_n = z_{n+2}$ for all $n \ge m+2$. It turns out that the orbit points z_n's for $n \ge m+2$ satisfy two coupled equations which read

$$\frac{d}{d\epsilon} z_n = \left(1 - \epsilon^2 \prod_{k=0}^{1} (1 - 2z_{n+k})^{-1}\right)^{-1} \sum_{N=0}^{1} \epsilon^N \left(\prod_{k=0}^{N} (1 - 2z_{n+k})^{-1}\right) z_{n+1+N}.$$

When $0 \le n \le m+1$, orbit points z_n's are governed by the following differential equations (see [6]):

$$\begin{aligned}\frac{d}{d\epsilon} z_n &= \sum_{N=0}^{m+1-n} \epsilon^N \left(\prod_{k=0}^{N} (1 - 2z_{n+k})^{-1}\right) z_{n+1+N} \\ &+ \left(1 - \epsilon^2 \prod_{k=0}^{1} (1 - 2z_{m+2+k})^{-1}\right)^{-1} \sum_{N=0}^{1} \epsilon^{m+2-n+N} \left(\prod_{k=0}^{m+2-n+N} (1 - 2z_{n+k})^{-1}\right) z_{m+3+N}.\end{aligned}$$

Hence, with the initial condition taken in this subsection, (3) reduces to a system of $(m+4)$-coupled ODEs.

We set $m = 12$. Figures 1 (a)$\sim$(g) show approximations of the Julia set $J(f_{1/\epsilon})$ by plotting the union of solutions $\bigcup_{n=0}^{15} z_n^*(\epsilon)$ for six different values of ϵ integrated along the ray $\mathcal{R}^+(1/6; M_\mu^{-1})$. The six values of ϵ are (a) 0, (b) $0.129889641 + 0.141065491i$, (c) $0.233392345+0.176828347i$, (d) $0.312689831+0.154912018i$, (e) $0.312597233+0.150118104i$, (f) $\frac{-i+i\sqrt{1-4i}}{4}$.

4.2 External angle 1/128

Here, we demonstrate how (3) can be employed to obtain periodic orbits for one of the Misiurewicz points of angle 1/128, $\epsilon \approx 0.567999678 + 0.348835133i$. We choose our initial condition for (5) to be

$$\begin{aligned}&\{z_0^*(0), z_1^*(0), \ldots, z_{97}^*(0)\} = \\ &\quad \{\ 0,1,0,0,0,1,1,0,1,1,0,0,0,0,0,1,0,1,0,0,1,1,1,0,0,1,0,1,1,1, \\ &\qquad 0,1,1,1,0,0,0,0,0,0,0,1,0,0,1,0,0,0,1,1,0,1,0,0,0,1,0,1,0,1, \\ &\qquad 1,0,0,1,1,1,1,0,0,0,1,0,0,1,1,0,1,0,1,0,1,1,1,1,0,0,1,1,0,1, \\ &\qquad 1,1,1,0,1,1,1,1\},\end{aligned}$$

and perform the numerical integration along the parameter ray $\mathcal{R}^+(1/128; M_\mu^{-1})$.

Table 1 displays the orbit points together with the numerical errors for the obtained period-98 orbit. It is clear that the errors are within the order of 10^{-5}.

References

[1] S. Aubry and G. Abramovici, *Chaotic trajectories in the standard map: the concept of anti-integrability*, Physica D, 43 (1990), pp. 199–219.

[2] L. Carleson and T. W. Gamelin, *Complex Dynamics*, Springer-Verlag, New York, 1993.

[3] Y.-C. Chen, *Bernoulli shift for second order recurrence relations near the anti-integrable limit*, Discrete Contin. Dyn. Syst. B, 5 (2005), pp. 587–598.

[4] Y.-C. Chen, *Smale horseshoe via the anti-integrability*, Chaos Solitons & Fractals, 28, (2006), pp. 377–385.

[5] Y.-C. Chen, *Anti-integrability for the logistic maps*, Chinese Ann. Math. B, 28 (2007), pp. 219–224.

[6] Y.-C. Chen, *Family of invariant Cantor sets as orbits of differential equations*, Int. J. Bifurcat. Chaos, 18 (2008), pp. 1825-1843.

[7] Y.-C. Chen, T. Kawahira, H.-L. Li, and J.-M. Yuan, (2009) 2D and 3D animations available online at http://www.math.sinica.edu.tw/ycchen/Animations/.

[8] Y.-C. Chen, T. Kawahira, H.-L. Li, and J.-M. Yuan, *Family of invariant Cantor sets as orbits of differential equaitons. II: Julia sets*, (2010), Preprint.

[9] A. Douady and J. H. Hubbard, *Iteration des polynomes quadratiques complexes*, C. R. Acad. Sci. Paris Ser. I Math., 294 (1982), pp. 123–126.

[10] A. Douady and J. H. Hubbard, *Etude dynamique des polynomes complexes. Partie I*, Publications Mathematiques d'Orsay, 84-2, 1984.

[11] T. Kawahira, *OTIS*, (2008), Java applet, available online at http://www.math.nagoya-u.ac.jp/~kawahira/programs/otis.html.

[12] M. LYUBICH, *Some typical properties of the dynamics of rational mappings*, Russian Math. Surveys, 38 (1983), pp. 154–155.

[13] R. S. MACKAY AND J. D. MEISS, *Cantori for symplectic maps near the anti-integrable limit*, Nonlinearity, 5 (1992), pp. 149–160.

[14] R. MAÑÉ, P. SAD, AND D. SULLIVAN, *On the dynamics of rational maps*, Ann. Sci. Ecole Norm. Sup., (4) 16 (1983), pp. 193–217.

[15] J. MILNOR, *Dynamics in One Complex Variable*, 3rd ed., Annals of Mathematics Studies, 160, Princeton University Press, Princeton, NJ, 2006.

[16] S. MOROSAWA, Y. NISHIMURA, M. TANIGUCHI AND T. UEDA, *Holomorphic Dynamics*, Cambridge University Press, Cambridge, 2000.

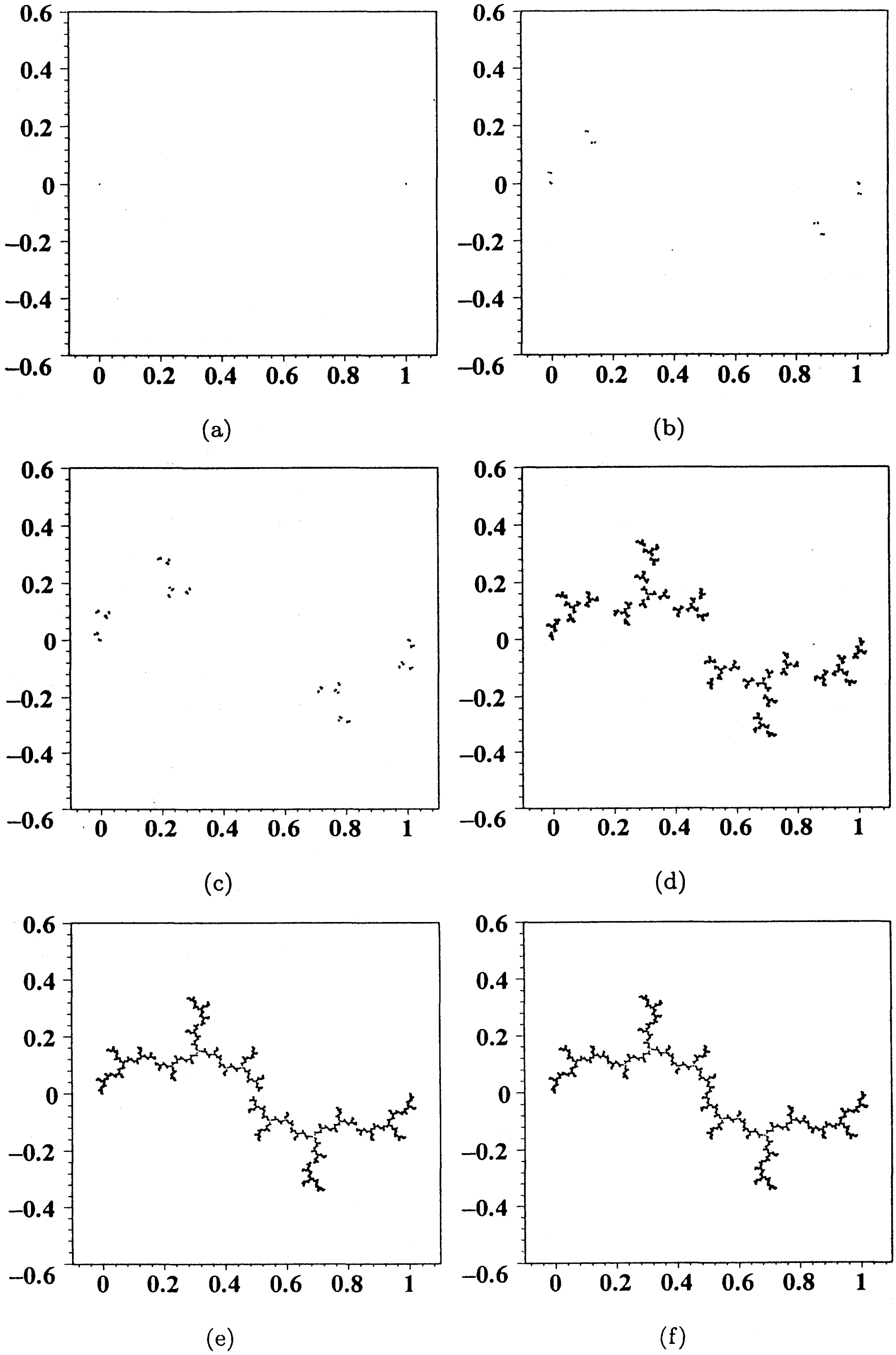

Figure 1: The Julia set $J(f_{1/\epsilon})$ for six different values of ϵ along $\mathcal{R}^+(1/6; M_\mu^{-1})$. See also the accompanying 3-D and 2-D animations online [7] for the numerical solutions.

Table 1: In the table $Error_n = |z_{n+1} - \epsilon^{-1} z_n(1 - z_n)|$.

n	z_n	$Error_n$
0	$0.2219225 + 0.7025727i$	6.3875180E-05
1	$1.1585066 - 0.0235395i$	1.4414667E-05
2	$-0.2097154 + 0.1833763i$	2.8986387E-05
3	$-0.0769903 + 0.5055563i$	6.4765670E-05
4	$0.6787778 + 0.6103129i$	3.8167939E-05
5	$0.5836139 - 0.7425738i$	5.3941587E-05
6	$1.1130641 - 0.4649153i$	6.2775251E-05
7	$0.5629855 + 0.6579069i$	3.8906294E-05
8	$0.8028143 - 0.6389108i$	6.2640044E-05
9	$1.0279777 + 0.0499355i$	3.9182835E-06
10	$-0.0749811 - 0.0467890i$	6.8983769E-06
11	$-0.1424939 - 0.0072215i$	1.2897096E-05
12	$-0.2153507 + 0.1159154i$	2.6035531E-05
13	$-0.1872256 + 0.4069632i$	5.8673982E-05
14	$0.3667061 + 0.7596082i$	5.9770305E-05
15	$1.1934887 - 0.3764129i$	5.5542720E-05
16	$0.2957900 + 0.7375319i$	6.1304841E-05
17	$1.1981355 - 0.2054721i$	2.8469686E-05
18	$-0.0242742 + 0.5200233i$	6.3262148E-05
19	$0.7420300 + 0.5043344i$	3.1391820E-05
20	$0.3782347 - 0.6620753i$	4.1770666E-05
21	$0.7344504 - 0.7348769i$	6.3818769E-05
22	$1.2102211 - 0.1365538i$	2.5666153E-05
23	$-0.1491321 + 0.4330886i$	5.7710326E-05
24	$0.4621315 + 0.7061330i$	4.7823637E-05
25	$0.9971740 - 0.5182167i$	6.1895721E-05
26	$0.7514826 + 0.4457438i$	2.8202094E-05
27	$0.3167554 - 0.5892330i$	3.5711366E-05
28	$0.5510044 - 0.7185475i$	4.9312520E-05
29	$1.0338513 - 0.5058499i$	6.2352731E-05
30	$0.7064254 + 0.5170933i$	2.8064090E-05
31	$0.4393642 - 0.6456632i$	3.8444416E-05
32	$0.7863752 - 0.6207580i$	6.1844916E-05
33	$0.9864725 + 0.0201376i$	1.3008316E-06
34	$0.0021955 - 0.0358438i$	2.1681250E-06
35	$-0.0235755 - 0.0483518i$	3.6743668E-06
36	$-0.0676149 - 0.0476191i$	6.4670736E-06
37	$-0.1318322 - 0.0142150i$	1.2083946E-05
38	$-0.2046071 + 0.0940290i$	2.4355368E-05
39	$-0.1997678 + 0.3559783i$	5.4860336E-05
40	$0.2467300 + 0.7256318i$	6.4517541E-05
41	$1.1992639 - 0.0893727i$	2.3756693E-05
42	$-0.1971714 + 0.3411496i$	5.3447602E-05
43	$0.2204670 + 0.7021034i$	6.3964363E-05
44	$1.1580259 - 0.0201055i$	1.4481666E-05
45	$-0.2126643 + 0.1771905i$	2.9142347E-05
46	$-0.0912774 + 0.5007116i$	6.5087707E-05
47	$0.6580502 + 0.6383887i$	4.0768346E-05
48	$0.6502528 - 0.7545769i$	6.0267661E-05
49	$1.1966416 - 0.3356524i$	5.3086075E-05
50	$0.2103574 + 0.6941909i$	6.4301186E-05
51	$1.1440918 + 0.0053744i$	1.2972271E-05
52	$-0.2161586 + 0.1205603i$	2.6179199E-05
53	$-0.1819294 + 0.4157538i$	5.8981657E-05
54	$0.3912507 + 0.7580534i$	5.8182569E-05
55	$1.1685276 - 0.4273271i$	5.8966289E-05
56	$0.4302632 + 0.7417198i$	5.3263175E-05
57	$1.0978909 - 0.4920903i$	6.4197221E-05
58	$0.6341584 + 0.6465697i$	4.0244363E-05
59	$0.6948383 - 0.7321181i$	6.0425768E-05
60	$1.1802352 - 0.2225318i$	2.6466541E-05
61	$0.0290513 + 0.5151846i$	5.9220737E-05
62	$0.7563540 + 0.3898687i$	2.5085521E-05
63	$0.2729780 - 0.5195723i$	3.0329039E-05
64	$0.4136317 - 0.6693413i$	4.0814691E-05
65	$0.7920460 - 0.6899405i$	6.4270209E-05
66	$1.1354542 + 0.0121828i$	1.2292203E-05
67	$-0.2085970 + 0.1008453i$	2.4749552E-05
68	$-0.1971045 + 0.3726714i$	5.5677737E-05
69	$0.2838202 + 0.7404911i$	6.2588372E-05
70	$1.2121601 - 0.1807470i$	2.9190269E-05
71	$-0.0848946 + 0.5053958i$	6.5242058E-05
72	$0.6729565 + 0.6276282i$	4.0514142E-05
73	$0.6145108 - 0.7595809i$	5.8821381E-05
74	$1.1769789 - 0.4165227i$	5.8631822E-05
75	$0.3982546 + 0.7483376i$	5.7346698E-05
76	$1.1418124 - 0.4330971i$	5.6980690E-05
77	$0.4692519 + 0.6906166i$	4.6614772E-05
78	$0.9614469 - 0.5156618i$	5.8903453E-05
79	$0.7609685 + 0.3705734i$	2.6060172E-05
80	$0.2562487 - 0.4979062i$	3.1130695E-05
81	$0.3700267 - 0.6545749i$	4.1230461E-05
82	$0.7121826 - 0.7369043i$	6.2316089E-05
83	$1.2017319 - 0.1874451i$	2.8353210E-05
84	$-0.0584713 + 0.4990813i$	6.3430289E-05
85	$0.6769645 + 0.5657264i$	3.3567951E-05
86	$0.5315292 - 0.6789118i$	4.6744796E-05
87	$0.9411586 - 0.5026027i$	5.6971729E-05
88	$0.7419056 + 0.3251555i$	2.3055403E-05
89	$0.2564449 - 0.4344726i$	2.6517874E-05
90	$0.3189469 - 0.5684711i$	3.3580652E-05
91	$0.5292255 - 0.6873913i$	4.6425232E-05
92	$0.9540823 - 0.5151739i$	5.8339503E-05
93	$0.7626346 + 0.3553978i$	2.6407905E-05
94	$0.2463359 - 0.4799620i$	3.1157386E-05
95	$0.3406883 - 0.6379125i$	4.0787600E-05
96	$0.6478187 - 0.7556505i$	6.0213525E-05
97	$1.1970073 - 0.3417854i$	5.3460189E-05